Referee comments are in black. Our responses are in blue.

The authors appreciate the comments made by the three referees. These comments, especially by Referee #1 and #3, motivated us to review the entrainment and scavenging efficiency calculations in terms of both the averages and uncertainties. As a result, there are several minor updates to the numbers presented in Tables S2 and S3. However, these changes do not affect the conclusions drawn in the submitted manuscript. Further, the comments posed by all three referees have strengthened the conclusions of the paper.

Anonymous Referee #1, 25 Feb 2026

This manuscript derives composition-specific aerosol scavenging efficiencies (SE) through the analysis of ten storms from the Deep Convective Clouds and Chemistry (DC3) and the Studies of Emissions, Atmospheric Composition, Clouds and Climate Coupling by Regional Surveys (SEAC$^4$RS) field experiments combined with process-scale modeling. The manuscript addresses an important problem—quantifying composition-dependent aerosol scavenging in deep convection—and provides a valuable observational dataset. The results presented can be used directly for evaluating cloud-scale chemistry transport model representation of aerosol scavenging.

The article is written clearly and would be a good contribution to ACP. However, the authors need to address the following comments before I can recommend publication in ACP.

**Major comments:**

The largest concern is the limited evaluation of uncertainty in entrainment rates and its propagation into scavenging efficiency (SE). Given that SE is directly dependent on the entrainment, a quantitative uncertainty analysis (e.g., sensitivity tests or error propagation) would substantially strengthen the robustness of the conclusions.

Entrainment rates used in this study are from the methodologies and results from our previous work (Fried et al., 2016; Barth et al., 2016; Cuchiara et al., 2020; Cuchiara et al., 2023). These papers discuss the methodologies and uncertainties in more detail. The impact of their uncertainties is now included in the manuscript and discussed further below, which has been added to the supplementary material (Text S1) and is cited in the manuscript (L232-234).

- Entrainment rates vary substantially among cases (Table S2), and different tracers were used to diagnose entrainment in different storms. While this is understandable given observational constraints, a more explicit discussion of the comparability of entrainment rates derived from different tracers would strengthen confidence in the results.

The entrainment rates were originally determined by previous work (Barth et al., 2016; Fried et al., 2016; Cuchiara et al., 2020; Cuchiara et al., 2023) where more details can be found. Here, we present the logic in choosing trace gases and list the trace gases used in the entrainment rate calculations as well as the entrainment rates determined from each trace gas for each storm case.

In choosing insoluble, passive trace gases for determining the entrainment rate in a storm, a few criteria are imposed. Insoluble trace gases generally have an effective Henry's Law constant of 1 M $atm^{-1}$ or less and include trace gases like CO, $O_3$, NO, $NO_2$, alkanes, and alkenes. Passive trace gases have a chemical lifetime much greater than the transport time from the inflow measurement location near cloud base to the outflow measurement location near cloud top. Based on model simulations where trajectories are launched near cloud base, the transport time ranges from 10-60 minutes (Skamarock et al., 2000; Bela et al., 2018). It is preferable to use insoluble, passive trace gases that have a substantial difference in mixing ratio between the boundary layer and the free troposphere. Many previous studies have used CO as the insoluble, passive trace gas because it is a fast-response measurement (1 Hz) with small uncertainty (5%), has a low Henry's Law constant ($9.8x10^{-4}$ at 298 K), long chemical lifetime (typically > 1 month), and often higher mixing ratios in the boundary layer than the free troposphere. However, because of its long chemical lifetime, its free troposphere mixing ratios are not necessarily much smaller than its boundary layer mixing ratios. Thus, when possible, i-butane, n-butane, i-pentane, and n-pentane are used for this analysis. These alkanes meet the criteria for being insoluble with a chemical lifetime of 1-5 days. However, their collection time via the whole air sampler method ranges from 45 s to a few minutes with longer collection times at high altitude. The sampling of convective outflows during SEAC$^4$RS were less than a minute. Thus, CO and $CO_2$ are used to calculate the entrainment rate for the SEAC$^4$RS storms, except for the marine convection on 18 September 2013 where the entrainment rate is from a WRF calculation that simulated tracers at 1-km altitude layers (for more information see Cuchiara et al., 2023). Table RR1 (which has been added to the supplement as Table S2) lists the trace gases used for the entrainment rate calculations. For most storm cases, the entrainment rate standard deviation is small compared to its average. More entrainment rate variation is seen for the 22 June 2012 and 18 September 2013 storms. Note that there is no systematic difference in entrainment rates when different trace gases are used (e.g., the entrainment rates using the alkanes as the passive, insoluble trace gas are 4 – 15% $km^{-1}$, while the entrainment rates using CO and $CO_2$ are 8 – 11% $km^{-1}$).

Table RR1. Trace gases used for the entrainment rate calculation for each storm and the entrainment rate average ± standard deviation among the 2-4 trace gases used for its calculation.

| Date | Insoluble, Passive Trace Gases | Entrainment Rate (% $km^{-1}$) |
|---|---|---|
| | *DC3* | |
| 18 May 2012 | i-,n-butane, i-,n-pentane | 14.7 ± 0.2 |
| 29 May 2012 | i-,n-butane, i-,n-pentane | 7.8 ± 0.9 |
| 02 June 2012 | CO | 11.5 |
| 06 June 2012 | i-,n-butane, i-,n-pentane | 4.1± 0.7 |

| | | |
|---|---|---|
| 16 June 2012 | i-,n-butane, i-,n-pentane | 15.4 ± 1.2 |
| 22 June 2012 | i-,n-butane, n-pentane | 5.5 ± 2.0 |
| | *SEAC$^4$RS* | |
| 02 Sept 2013 | CO, $CO_2$ | 11.4 ± 1.6 |
| 02 Sept 2013 | CO, $CO_2$ | 8.3 ± 1.6 |
| 18 Sept 2013 Marine | WRF tracer calculation | 9.6 ± 3.2 |
| 18 Sept 2013 Land, core 2 | CO, $CO_2$ | 7.8 ± 5.2 |
| 18 Sept 2013 Land, core 3 | CO, $CO_2$ | 10.4 ± 5.4 |

- It would be helpful to show the vertical profiles of the tracers used to derive entrainment alongside the corresponding aerosol vertical profiles, to assess how similar their vertical structures are and how sensitive the entrainment correction may be to profile heterogeneity.

The vertical profiles of the passive, insoluble tracer gases used to derive entrainment rates have been added to Fig. 2 (shown below), which shows the clear sky vertical profiles.

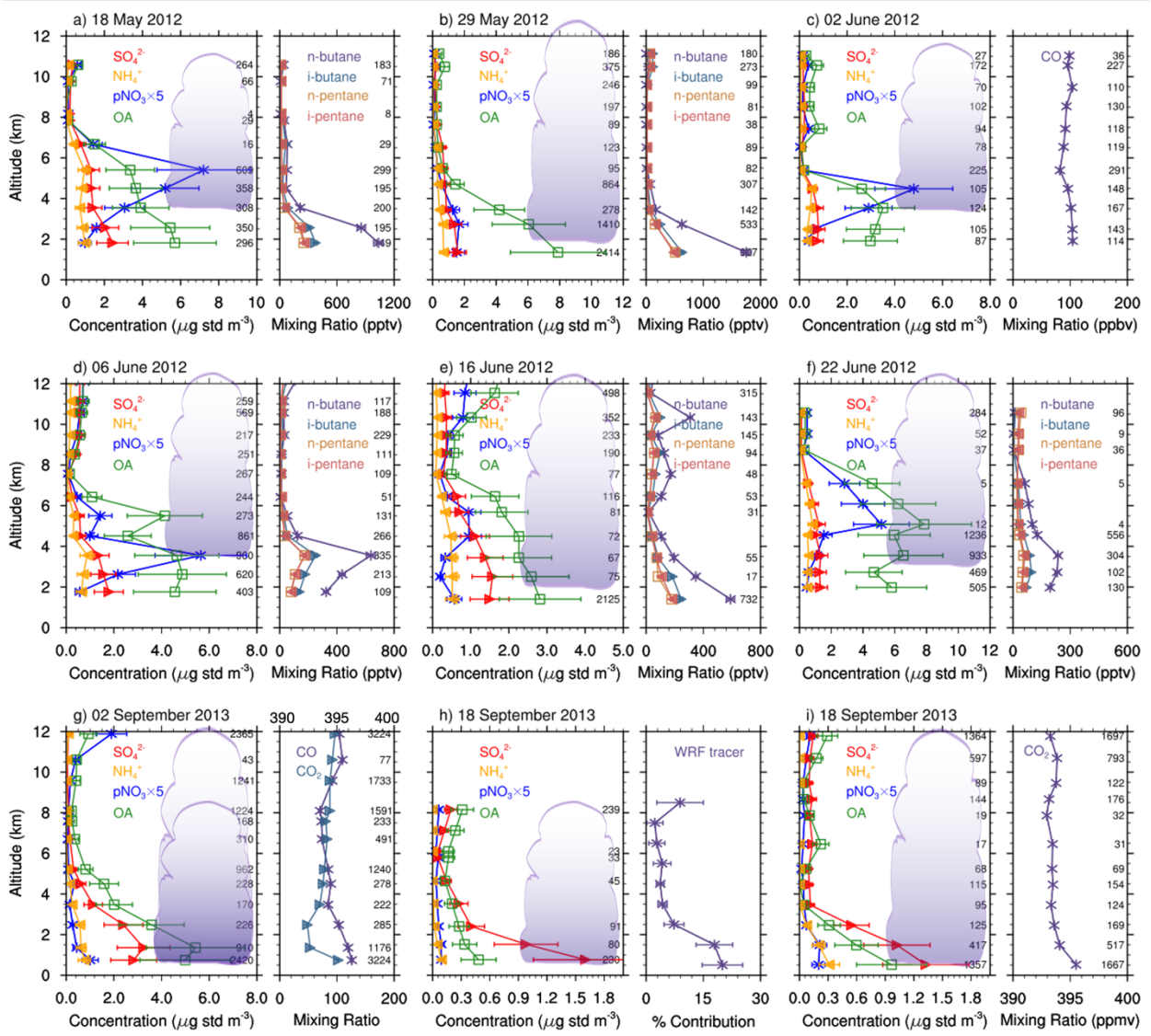


Figure 2. Clear air vertical profiles of sulfate (red with right arrows), particulate nitrate (blue with asterisks), ammonium (gold with left arrows), organic aerosol (green with squares), and the passive, insoluble trace gases used in the entrainment model for a) 18 May 2012, b) 29 May 2012, c) 2 June 2012, d) 6 June 2012, e) 16 June 2012, f) 22 June 2012, g) 2 September 2013, h) 18 September 2013 over the Gulf of Mexico, and i) 18 September 2013 over South Texas. Average and standard deviations are plotted for each altitude bin, which is plotted at the average altitude of each 1-km bin. The number of samples included in each altitude bin is listed on the right side of the panel. Nitrate concentrations shown are multiplied by a factor of 5 for visibility. In g), the $CO_2$ mixing ratio (ppmv) axis is at the top of the panel. The cloud schematic in each panel is used to locate the approximate cloud base and cloud top heights for each case. Cloud tops extending above the panel indicate that the actual cloud top was much greater than 12 km and is noted in Table 1. In g) two cloud tops are shown, ~8 km for the airmass storm and ~13 km for the multicell storm.

- More importantly, the manuscript does not quantify how uncertainty in entrainment rates and in the clear-air and outflow aerosol profiles propagates into SE uncertainty. In Table S2, only cases with multiple outflow legs include standard deviations, while other cases appear to lack uncertainty bounds.

The reviewer's point about discussing uncertainty in the results is well taken, resulting in this information being added to the paper (L400-407; Tables S2, S3; Fig. 3). An analysis of the entrainment rate among passive tracers for each storm shows that there is often a small variation, although a couple of storm cases have a larger variation (see Table RR2). The 1-sigma uncertainty (accuracy, not precision) in the AMS measurements is 17% of the measurement value for the inorganics and 19% for organic aerosol (Bahreini et al., 2009) and is discussed in more detail in the response to Referee #3. The AMS measurement uncertainty propagates to an uncertainty in the derived scavenging efficiencies that is larger than the uncertainty from the entrainment rate variation in all cases except for the land convection on 18 September 2013.

The 18 May 2012 DC3 case is used to give an example. For that case, the entrainment rate is 14.7 ± 0.2 % $km^{-1}$ where the variability is equal to the largest deviation of the individual entrainment rate from the average entrainment rate. Calculating the $SO_4^{2-}$ SE using entrainment rates of 14.9 % $km^{-1}$ and 14.5 % $km^{-1}$ results in a 62.9 ± 0.6% scavenging efficiency. In contrast, propagating the 17% measurement uncertainty to the calculation of $SO_4^{2-}$ SE results in 62.9 ± 7.4% scavenging efficiency. Therefore, we now report in Table S3 and Fig. 3 the scavenging efficiency uncertainties as the maximum of the propagation of the uncertainty of the AMS measurements or standard deviation from the entrainment rate variability.

Table RR2. Entrainment rates ± standard deviation and scavenging efficiencies (SE) ± uncertainty based on uncertainty of measurement for each storm case. The entrainment rate standard deviation is equal to the maximum difference between the highest or lowest entrainment rate minus the average entrainment rate. For cases where the outflow leg is below the detection limit, the scavenging efficiency is shown as 100% and an uncertainty is not assigned since the measured outflow concentration is not statistically different than zero.

| Storm | Entrainment Rate | $SO_4^{2-}$ SE | $NH_4^+$ SE | $NO_3^-$ SE | OA SE |
|---|---|---|---|---|---|
| 18 May 2012 | 14.7 ± 0.2 | 62.9 ± 7.4 | 39.2 ± 12.0 | – | 28.9 ± 15.8 |
| 29 May 2012 | 7.8 ± 0.9 | 86.8 ± 3.2 | 81.3 ± 4.6 | 40.5 ± 13.7 | 84.5 ± 4.4 |
| 02 June 2012 | 11.5 | 56.5 ± 8.4 | 37.0 ± 12.3 | – | 48.0 ± 11.7 |
| 06 June 2012 | 4.1± 0.7 | 89.6 ± 2.5 | 86.0 ± 3.4 | 41.9 ± 10.6 | 86.7 ± 3.6 |
| 16 June 2012 | 15.4 ± 1.2 | 90.7 ± 1.9 | 87.6 ± 2.5 | 82.8 ± 3.1 | 89.5 ± 2.3 |
| 22 June 2012 | 5.5 ± 2.0 | 75.2 ± 7.9 | 65.3 ± 9.7 | – | 66.2 ± 11.1 |
| 02 Sept 2013, airmass | 11.4 ± 1.6 | 95.0 ± 1.2 | 100 | 42.9 ± 13.5 | 84.4 ± 4.0 |
| 02 Sept 2013, multicell | 8.3 ± 1.6 | 92.7 ± 1.9 | 80.9 ± 4.9 | – | 57.6 ± 11.7 |
| 18 Sept 2013 | 9.6 ± 3.2 | 100 | 100 | NaN | 100 |
| 18 Sept 2013, land core 2 | 7.8 ± 5.2 | 90.7 ± 4.9 | 100 | 100 | 100 |
| 18 Sept 2013, land, core 3 | 10.4 ± 5.4 | 87.9 ± 7.0 | 100 | 100 | 100 |

The discussion focuses primarily on chemical processes and entrainment of mid-free-tropospheric aerosol layers in interpreting SE variability. However, the dynamical controls on scavenging are less clearly developed. Although SE is shown as a function of the SWEAT index, the analysis does not fully explore how dynamical factors (e.g., convective intensity and updraft strength) may influence the observed chemical and scavenging signatures. The connection between storm dynamics and composition-dependent SE could be developed further, particularly in the Conclusions section.

The SWEAT index combines thermodynamic and dynamic factors and provides an indication of convective intensity. The SWEAT index is useful with aircraft measurements as near-surface data are not needed for its calculation. Comparison of scavenging efficiencies to individual parameters show a strong correlation of scavenging efficiency with CAPE but a weak correlation with the 0-6 km shear for the DC3 storms, suggesting that the thermodynamics plays a stronger role. We also found a moderately strong correlation with the depth of the cloud base to the freezing level for the DC3 storms, which is an indication that nucleation scavenging controls the transport efficiency to the upper troposphere. There is no strong correlation of these other meteorological parameters with the SEAC$^4$RS storms because of other factors, which include using the same NWS sounding for each date and several outflow concentrations being less than the detection limit. Scavenging efficiency also did not have a strong correlation with the volume of the 35 dBZ region of the storm (not shown). These comments are now included in the manuscript (389-397) and Fig. RR1 below has been added to the supplement as Fig. S2.

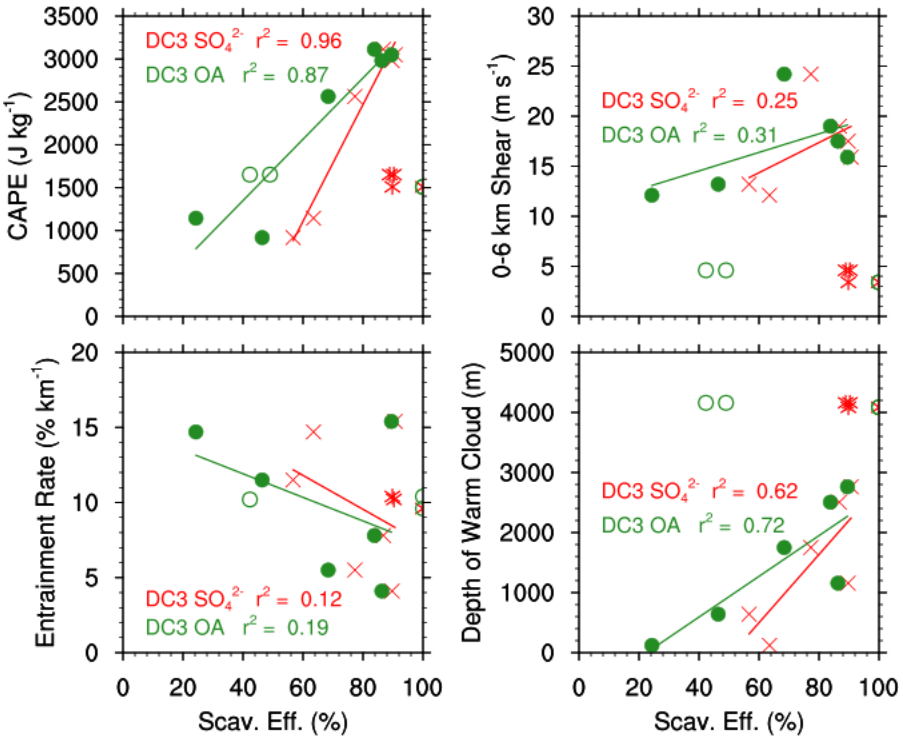

Figure RR1. Scatter plots of $SO_4^{2-}$ (red) and OA (green) scavenging efficiencies with various storm parameters (upper left: CAPE; upper right: 0-6 km wind shear; lower left: entrainment rate; lower right: depth from cloud base to 0°C). The CAPE, wind shear, and warm cloud depth are from DC3 radiosondes or NWS radiosondes. The correlation coefficients are based on only the DC3 storms.

**Minor comments:**

Tick directions are inconsistent across figures. For example, Fig. 4 and Fig. 6 have inward ticks, while other figures use outward ticks. Please standardize formatting.

The figure formatting is more standardized.

Figure 2: It would be helpful to include the sample size (e.g., number of seconds of sampling) within each 1-km bin for the clear-air vertical profiles. Additionally, the method used to define the inflow aerosol concentration below cloud base should be clarified. Was the bin closest to cloud base used, or was an average taken across all sub-cloud layers?

The number of measurements contributing to each sample has been added to the figure (see above).

The inflow aerosol concentrations are taken from the pre-defined time period used in previous studies (Table S3, which also lists the altitude of the inflow). This is already stated in Section 3 in lines 239-242 of the original submitted paper, but is now noted earlier in that section as well (L225-227). In contrast, the clear air vertical profiles include all measurements within the 0-1 km or 1-2 km altitude bins.

Line 381: It would strengthen the discussion to provide references and typical magnitudes for below-cloud scavenging efficiency for comparison.

We now cite Flossmann (1991) who found 90% of the aerosol mass scavenged is incorporated into cloud water via nucleation scavenging, and ~30% of the aerosol in rain at the ground is due to below cloud impaction scavenging (L420-422).

The Conclusions section would benefit from a brief, explicit statement of the main limitations of the study (e.g., entrainment uncertainty, tracer dependence, simplified chemical interpretation).

We have added the following paragraph to the Conclusions section (L653-663).

The conclusions from this analysis are limited by a number of factors. The uncertainties associated with the scavenging efficiency calculations due to the uncertainties in the aerosol concentration measurements, the derived entrainment rates, and the estimated inflow and outflow time periods. This paper attempts to quantify these uncertainties, which are mostly < 10% of the average for sulfate and ammonium scavenging efficiencies and < 16% for particulate nitrate and organic aerosol scavenging efficiencies. Explanations for why particulate nitrate scavenging efficiencies are lower for some cases are based on simple calculations of entrainment effects and potential impacts of lightning-produced nitrogen oxides. Detailed cloud-resolving chemistry

transport modeling can extend our knowledge for both these processes (e.g., Cummings et al., 2024; Pickering et al., 2024). Likewise, the explanations for why organic aerosol scavenging efficiencies are lower in some cases are based on simple parcel model calculations of the aqueous-phase production of organic acids. A more complete representation of gas and aqueous phase chemistry coupled with aerosol thermodynamics and SOA formation in a cloud-resolving chemistry transport model would provide better quantification of the contribution of aqueous-phase chemistry.

## References


Bahreini, R., Ervens, B., Middlebrook, A. M., Warneke, C., de Gouw, J. A., DeCarlo, P. F., Jimenez, J. L., Brock, C. A., Neuman, J. A., Ryerson, T. B., Stark, H., Atlas, E., Brioude, J., Fried, A., Holloway, J. S., Peischl, J., Richter, D., Walega, J., Weibring, P., Wollny, A. G., Fehsenfeld, F. C.: Organic aerosol formation in urban and industrial plumes near Houston and Dallas, Texas, J. Geophys. Res., 114, D00F16, doi:10.1029/2008JD011493, 2009.

Barth, M. C., Bela, M. M., Fried, A., Wennberg, P., Crounse, J., St. Clair, J., Blake, N., Blake, D. R., Homeyer, C. R., Brune, W. H., Zhang, L., Mao, J., Ren, X., Ryerson, T., Pollack, I. B., Peischl, J., Cohen, R. C., Nault, B. A., Huey, L. G., Liu, X., and Cantrell, C. A.: Convective Transport and Scavenging of Peroxides by Thunderstorms Observed over the Central U.S. during DC3, J. Geophys. Res., 121, 4272– 4295, doi:10.1002/2015JD024570, 2016.

Bela, M. M., Barth, M. C., Toon, O. B., Fried, A., Ziegler, C., Cummings, K. A., Li, Y., Pickering, K. E., Homeyer, C. R., Morrison, H., Yang, Q., Mecikalski, R. M., Carey, L., Biggerstaff, M. I., Betten, D. P., and Alford, A. A.: Effects of scavenging, entrainment, and aqueous chemistry on peroxides and formaldehyde in deep convective outflow over the central and Southeast U.S., J. Geophys. Res., 123, 7594– 7614, doi:10.1029/2018JD028271, 2018.

Cuchiara, G. C., Fried, A., Barth, M. C., Bela, M., Homeyer, C. R., Gaubert, B., Walega, J., Weibring, P., Richter, D., Wennberg, P., Crounse, J., Kim, M., Diskin, G., Hanisco, T. M., Wolfe, G. M., Beyersdorf, A., Peischl, J., Pollack, I. B., St. Clair, J. M., Woods, S., Tanelli, S., Bui, T. P., Dean-Day, J., Huey, G. L., and Heath, N.: Vertical transport, entrainment, and scavenging processes affecting trace gases in a modeled and observed SEAC$^4$RS case study. J. Geophys. Res., 125, e2019JD031957, doi:10.1029/2019JD031957, 2020.

Cuchiara, G. C., Fried, A., Barth, M. C., Bela, M., Homeyer, C. R., Walega, J., Weibring, P., Richter, D., Woods, S., Beyersdorf, A., Bui, T. P., Dean-Day, J.: Effect of marine and land convection on wet scavenging of ozone precursors observed during a SEAC$^4$RS case study, J. Geophys. Res., 28, e2022JD037107, doi:10.1029/2022JD037107, 2023.

Cummings, K. A., Pickering, K. E., Barth, M. C., Bela, M. M., Li, Y., Allen, D., Bruning, E., MacGorman, D. R., Ziegler, C. L., Biggerstaff, M. L., Fuchs, B., Davis, T., Carey, L.,

Mecikalski, R. M., and Finney, D. L.: Evaluation of lightning flash rate parameterizations in a cloud-resolved WRF-Chem simulation of the 29–30 May 2012 Oklahoma severe supercell system observed during DC3. J. Geophys. Res.,, 129, e2023JD039492. doi:10.1029/2023JD039492, 2024.

Flossmann, A. I.: The scavenging of two different types of marine aerosol particles calculated using a two-dimensional detailed cloud model, Tellus, 43B, 301-321, doi:10.1034/j.1600-0889.1991.t01-2-00004.x, 1991.

Fried, A., Barth, M. C., Bela, M., Weibring, P., Richter, D., Walega, J., Li, Y., Pickering, K. E., Apel, E., Hornbrock, R. S., Hills, A., Riemer, D. D., Blake, N., Blake, D., Schroeder, J. R., Luo, Z. J., Crawford, J. H., Olson, J., Rutledge, S., Betten, D., Biggerstaff, M. I., Diskin, G., Sachse, G., Campos, T., Flocke, F., Weinheimer, A., Cantrell, C., Pollack, I., Peischl, J., Froyd, K., Wisthaler, A., Mikoviny, T. and Woods, S.: Convective Transport of formaldehyde to the upper troposphere and lower stratosphere and associated scavenging in thunderstorms over the Central United States during the 2012 DC3 study, J. Geophys. Res., 120, 7430– 7460, doi:10.1002/2015JD024477, 2016.

Pickering, K. E., Li, Y., Cummings, K. A., Barth, M. C., Allen, D. J., Bruning, E. C., and Pollack, I. B.:Lightning $NO_x$ in the 29–30 May 2012 Deep Convective Clouds and Chemistry (DC3) severe storm and its downwind chemical consequences, J. Geophys. Res., 129, e2023JD039439, doi:10.1029/2023JD039439, 2024.

Skamarock, W. C., Powers, J. G., Barth, M., Dye, J. E., Matejka, T., Bartels, D., Baumann, K., Stith, J., Parrish, D. D., Hubler, G.: Numerical simulations of the July 10 Stratospheric-Tropospheric Experiment: Radiation, Aerosols, and Ozone/Deep Convection Experiment convective system: Kinematics and transport, J. Geophys. Res., 105, 19,973-19,990, doi:10.1029/2000JD900179, 2000.